POULTRY CRC LTD

FINAL REPORT

Sub-Project No: 2.9.1.

PROJECT LEADER: Sandra G. Velleman

Sub-Project Title: Changes in Broiler Breast Muscle with the "Wooden" Breast Myopathy

DATE OF COMPLETION: 5 February 2016

ISBN 1 921010 88 6

Changes in Broiler Breast Muscle with the "Wooden" Breast Myopathy
Sub-Project No. 2.9.1

Researcher Contact Details
Name: Sandra G. Velleman
Address: 1680 Madison Ave.

Phone: 330-263-3905
Fax: 330-263-3949
Email: Velleman.1@osu.edu

In submitting this report, the researcher has agreed to the Poultry CRC publishing this material in its edited form.

Poultry CRC Ltd Contact Details
PO Box U242
University of New England
ARMIDALE NSW 2351

Phone: 02 6773 3767
Fax: 02 6773 3050
Email: admin@poultrycrc.com.au
Website: http://www.poultrycrc.com.au

Published in 2016

INTRODUCTION

Consumer demand for poultry products has substantially increased over the last 50 yrs and is expected to continue to rise (OECD-FAO, 2015). The poultry industry has increased broiler production by selecting for growth, muscle mass accretion including pectoralis major muscle (**p. major**) or breast muscle yield, and feed conversion. Breast muscles from meat-type commercial broilers are 10 times larger than those from broilers marketed in 1955 at the same age (Collins et al., 2014). The incidence of myopathies in the p. major muscle has increased with growth (Dransfield and Sosnicki, 1999; Velleman, 2015). Myopathies such as wooden breast (**WB**) (Zotte et al., 2014; Kindlein et al., 2015; Mudalal et al., 2015; Velleman and Clark, 2015), white striping (Kuttappan et al., 2013; Petracci et al., 2013), deep pectoral myopathy (Siller, 1985; Richardson et al., 1980; Kijowski and Konstanczak, 2009), and pale, soft and exudative meat (Van Laack et al., 2000; Woelfel et al., 2002) reduce meat quality by negatively impacting water-holding capacity, textural properties, and visual appearance.

The WB myopathy is associated with fast growing broilers and heavy p. major weights (Zotte et al., 2014; Kindlein et al., 2015; Mudalal et al., 2015; Velleman and Clark, 2015). Kindlein et al. (2015) have estimated WB to affect up to 32% of current commercial broilers at 35 d of age and up to 89% of commercial broilers by 42 d of age. Bailey et al. (2015) reported a very low heritability coefficient (0.02 to 0.10) for the WB myopathy in two moderate to high yielding broiler lines. A low heritability would suggest that the WB myopathy has a strong non-genetic or environmental component. Wooden breast reduces the value of the breast meat and is phenotypically identified by the palpation of a rigid, non-pliable p. major muscle (Sihvo et al., 2013). Further processing yield and finished product quality are also affected as WB meat has

reduced water-holding capacity and manifests poor texture (Mazzoni et al., 2015; Mudalal et al., 2015).

The WB myopathy was first described by Sihvo et al. (2013) in p. major muscles that were “remarkably hardened diffusely or on focally extensive areas” with a sterile exudate, hemorrhaging over the surface of the muscle, and a pale, undesirable breast muscle color (Sihvo et al., 2013, Bailey et al., 2015). Wooden breast affected muscle is structurally characterized by varying degrees of fiber necrosis, fibrosis, small regenerating fibers, immune cell infiltration, and extensive fibrillar collagen deposition (Sihvo et al. 2013; Velleman and Clark, 2015). Velleman and Clark (2015) also reported differential expression of decorin in WB affected and unaffected breast muscle in broilers from different lines. Decorin is a small leucine-rich proteoglycan with multiple physiological functions including but not limited to regulation of transforming growth factor beta (**TGF-β**) signaling (Schönherr et al., 1998; Riquelme et al., 2001; Brandan et al., 2008) and collagen crosslinking (Weber et al., 1996; Danielson et al., 1997). Consequently, decorin is critically important for proper cellular growth, collagen fibril structure, and extracellular matrix organization.

Myogenesis and muscle growth has distinct embryonic and posthatch phases. Embryonic skeletal muscle formation occurs through the proliferation and differentiation of myoblasts which fuse to form multinucleated myotubes and then differentiate into muscle fibers. The formation of muscle fibers, also termed hyperplastic growth, is complete at hatch (Smith, 1963). Subsequent muscle growth occurs through the enlargement or hypertrophy of existing fibers as myoblasts are withdrawn from the cell cycle after fusing to form multinucleated myotubes. Posthatch muscle growth is mediated by an adult myoblast stem cell population termed satellite cells which are located between the basement membrane and sarcolemma of skeletal muscle

fibers (Mauro, 1961). Satellite cells contribute to hypertrophy by fusing with, and donating their nuclei to existing muscle fibers, leading to myonuclear DNA accretion (Stockdale and Holtzer, 1961; Moss and LeBlond, 1971) and the potential for increased protein synthesis and muscle fiber growth through hypertrophy.

Selection for increased p. major muscle mass accretion has increased muscle fiber size through posthatch hypertrophic growth (Dransfield and Sosnicki, 1999; Scheuermann et al., 2004). Large hypertrophic myofibers could create circulatory challenges which have negative implications for meat quality (Berri et al., 2007) due to less perimysial and endomysial connective tissue space. A reduction in the endomysium or perimysium restricts the amount of space available for blood supply and capillaries to the muscle (Wilson et al., 1990, Hoving-Bolink et al., 2000; Velleman et al., 2003a). With decreased endoymysial and perimysial connective spacing, the risk of muscle fiber damage increases (Wilson et al., 1990; Velleman et al., 2003a) which activates satellite cell mediated muscle fiber repair mechanisms (Velleman et al., 2003a). In addition, with reduced capillaries, lactic acid, a by-product of anaerobic respiration, is not effectively removed from the breast muscle leading to further muscle damage and ultimately detrimental effects on meat quality (Sandercock et al., 2001). Satellite cells are also dependent upon the vasculature system for their activity. Satellite cells often proliferate in close proximity to capillaries (Christov et al., 2007) and recent studies suggest that satellite cell activation requires signaling from vascular cells (Christov et al., 2007, Rhoades et al., 2009; 2013). Due to this, without adequate circulation satellite cell function and muscle regeneration will be hindered (Luque et al., 1995; Christov et al., 2007, Rhoades et al., 2009), thereby affecting posthatch muscle growth. Taken as a whole, these studies suggest that a reduction or

loss of blood supply to the muscle will likely lead to a build-up of metabolic waste products and negatively impact satellite cell function, possibly causing the onset of muscle myopathies.

Spatial differences in hyperplastic and hypertrophic growth are required to produce the p. major shape which may cause variations in muscle fiber size, fiber bundle organization, perimysial and endomysial connective tissue spacing, and circulatory supply availability to the muscle. The thickest portion of the p. major muscle, the anterior region, is over 350% thicker than the thinnest posterior area of the p. major muscle in commercial broilers (Mudalal et al., 2015). The p. major anterior thickness has increased with growth selection and is correlated to breast meat yield (Guernec et al., 2003). Broilers with the WB myopathy also have up to 30% thicker p. major muscles compared to unaffected broilers (Mudalal et al., 2015). It is likely that the increased anterior p. major muscle thickness contains larger myofibers. Increased myofiber size will limit endomysial and perimysial spacing available for capillaries and blood supply in the anterior region of the p. major muscle and increase the potential for muscle fiber damage. Satellite cell activity is dependent upon close proximity to the circulatory system (Christov et al., 2007). Reduced circulatory supply by limited endomysial and perimysial connective tissue spacing will suppress satellite cell mediated growth and regeneration of muscle fibers. Thus, these factors may be associated with the WB myopathy due to conditions increasing the potential for breast muscle necrosis and fibrosis.

In support of this hypothesis, WB is initially palpable in the anterior region of the p. major muscle of affected broilers, and can only be felt throughout the entire p. major muscle in severe cases (Bailey et al, 2015). The anterior p. major WB affected muscles also have a higher ultimate, postmortem pH compared to unaffected muscles; whereas the pH in the posterior p. major muscle are not affected by the WB myopathy (Zotte et al., 2014). These data suggest that

due to the temporal and spatial regulation of p. major muscle development and growth, the WB myopathy will differentially develop within the muscle. The primary objective of the present study was to determine morphological changes associated with WB in different regions of the p. major muscle. A secondary objective was to determine if there were differences in fiber size and morphology in WB affected and unaffected p. major muscle from different broiler lines.

MATERIALS AND METHODS

Birds

At approximately 40 d of age, p. major muscle samples were obtained from three commercial broiler lines (A, B, and C). Lines A and B were fast growing commercial broiler lines expressing the WB myopathy. Line C was a slower growing line that displayed no phenotypic occurrence of the WB condition. In total, 44 male birds were used in the study with 20 from Line A, 14 from Line B, and 10 from Line C. Birds were selected by experienced producer personnel that palpated the p. major muscle of live birds. From Line A, 10 birds were selected that had a hard, rigid p. major muscle and phenotypically determined to have WB, while 10 additional birds were selected that had a seemingly normal p. major muscle. From Line B, 4 birds were selected that had a hard, rigid p. major muscle while 10 birds were selected that had a seemingly normal p. major muscle. The p. major muscle from Line C broilers, as evaluated before slaughter, did not exhibit any phenotypic WB characteristics.

Sample Collection and Histology

Samples were taken from four locations throughout the p. major muscle. The samples were obtained from an anteroventral (**AV**) position, a ventral position in the middle (**MV**) of the p. major, a posteroventral (**PV**) position, and an anterodorsal (**AD**) position (Figure 1) of the p.

major muscle. Samples were taken from each position to evaluate spatial effects on p. major morphological structure and gene expression.

Immediately after euthanasia, the skin was removed to expose the p. major muscle. Between 100 and 200 mg p. major muscle samples were removed at each of the three ventral positions for RNA expression analysis. Samples for gene expression analysis were placed in RNAlater (Ambion, Grand Island, NY). Histological samples were obtained according to the procedure of Velleman et al. (2003a). In brief, a muscle sample oriented along the muscle fibers approximately 0.5 cm wide by 0.5 cm deep by 3 cm long was excised. Prior to removal, the ends of the sample were tied to a wooden applicator stick to prevent muscle contraction. The AD sample was excised by making a 2 cm incision proximal to the AV sample to expose a layer of p. major muscle that was 2 cm deep in the p. major muscle. Samples were removed for RNA and histology at this position as described. After excision, histology samples were placed in 10% (vol/vol) buffered formalin fixative pH 7.0 and stored at 4 °C. All samples were then shipped to the laboratory of Dr. Sandra Velleman at The Ohio State University/OARDC in Wooster, OH. Histological samples were dehydrated in a graded series of alcohols, cleared in Pro Par Clearant (Anatech, Battle Creek, MI) and paraffin embedded according to the procedure of Jarrold et al. (1999). Paraffin blocks were cross sectioned at 5 µm, mounted on Starfrost Adhesive slides (Mercedes Medical, Sarasota, FL), and hematoxylin and eosin stained as described by Jarrold et al. (1999). Each slide contained a minimum of four sections.

Digital photomicrographs were taken with an Olympus IX70 fluorescent microscope (Olympus America, Mellville, NY) and QImaging digital camera (QImaging, Burnaby, BC, Canada) equipped with CellSens Imaging software (Olympus America). From each sample, four photomicrographs were taken at 100x and 200x magnification for morphological score analysis

based upon the method of Velleman et al. (2003b). The four 100x images were displayed simultaneously to four trained panelists and scored for macrophage infiltration, fiber necrosis, and the microscopically observable amount of endomysial connective and perimysial connective tissue content. For macrophage infiltration, a score of 5 was given to samples with no to very few macrophages present whereas a score of 1 was given to samples with extensive macrophage infiltration in multiple images. For fiber necrosis, a score of 5 was given to samples with minimal to no fibers present within each photomicrograph that exhibited necrosis while a score of 1 was given to samples with extensive fiber necrosis in all four photomicrographs. For the amount of observable endomysial connective tissue between muscle fibers, a score of 5 was given to samples with a normal amount of endomysial content between individual muscle fibers whereas a score of 1 was given to samples with an extensive amount of endomysial content. For the amount of observable perimysial connective tissue content, a score of 5 was given to samples with a normal distribution of perimysial content, and a score of 1 was given to samples with an abundance of perimysial content.

Myofiber diameter was measured from 2 photomicrographs imaged at 200x. Diameters of all completely visible muscle fibers present within each photomicrograph were measured using Image Pro software (MediaCybernectics, Bethesda, MD). A minimum of 30 fiber diameters were measured per sample.

Total RNA Extraction and cDNA Synthesis

Total RNA was extracted from individual p. major muscle samples using RNAzol (Molecular Research Center, Cincinnati, OH) according to manufacturer's protocol. Moloney Murine Leukemia Virus Reverse Transcriptase (**M-MLV RT**; Promega, Madison, WI) was used to synthesize the cDNA. The reaction consisted of 1 µg of total RNA, 1 µl of 50 µM Oligo

$d(T)_{20}$ (Eurofins, Huntsville, AL), and nuclease-free water up to 13.5 µl. The reaction was then incubated at 80 °C for 5 min and then cooled on ice. After cooling, 5 µL of M-MLV RT 5x buffer (Promega), 1 µL of 10 *mM* deoxynucleoside triphosphate mix, 0.25 µL of RNasin (40 U/µL), 1 µL of M-MLV RT (200 U/µL), and 4.25 µL of nuclease-free water was added to the reaction. The reaction mixture was then incubated at 55 °C for 60 min and then 90 °C for 10 min to stop the reaction. After cDNA synthesis, 25 µL of nuclease-free water was added to the cDNA.

Real-Time Quantitative PCR

Expression of myogenic determination factor (***MYOD1***), myogenin, decorin, and insulin-like growth factor type 1 receptor (***IGF1R***) were measured by real-time quantitative PCR (**qPCR)** using DyNAmo Hot Start SYBR Green qPCR kit (Thermo Fisher Scientific, Waltham, MA) and a DNA Engine Opticon 2 real-time system (Bio-Rad, Hercules, CA). Reaction mixtures contained 18 µL DyNAmo Hot Start SYBR Green qPCR master mix (Thermo Fisher Scientific), 2 µL of cDNA, 1 µL of 10 µM 1:1 forward and reverse target primer mixture, and 7 µL of nuclease-free water. All samples were run in triplicate reactions. Primers for *MYOD1*, myogenin, decorin, *IGF1R* and glyceraldehyde-3-phosphate dehydrogenase (***GAPDH***) are listed in Table 1. Primer specificity was confirmed by sequencing the PCR products (Molecular and Cellular Imaging Center, The Ohio State University/Ohio Agricultural Research and Development Center, Wooster, OH). Thermocycler program conditions were: denaturation (94 °C for 15 min), amplification and quantification (35 cycles of 94 °C for 30 s, 58 °C [for *MYOD1* and myogenin], or 55 °C [for decorin, *IGF1R*, and *GAPDH*] for 30s, and 72 °C for 30s), and final extension at 72 °C for 5 min. The melting curve program was 52 °C to 95 °C with a reading taken every 0.2 °C and a 1-s hold. A standard curve for each gene was prepared using serial dilutions of purified

PCR products as previously described by Liu et al. (2006). The arbitrary amount of sample cDNA for each gene was interpolated from the corresponding standard curve. To standardize samples across plates and reduce plate to plate variation, two standardization control samples were run in triplicate on every plate. All samples were then standardized to the standardization control samples (**SCS**) by calculating the SCS mean for each plate and then obtaining a ratio by dividing the SCS mean for each plate by the SCS mean for all plates. Normalized arbitrary units were calculated by dividing the arbitrary molar concentration of the samples for each gene by the arbitrary *GAPDH* molar concentration. To ensure gene amplification specificity, randomly selected PCR products were resolved on a 1.0% agarose gel to verify the presence of a single band that corresponded to the correct molecular weight for each gene. As further confirmation, each sample and primer pair produced a single dissociation curve from the melting curve program. A no-template negative control was included in each qPCR reaction for the detection of contamination.

Statistical Analysis

Live birds were identified as normal or WB affected based upon live palpation. However, some birds that were identified as normal based upon palpation had microscopic morphologic symptoms such as macrophage infiltration, collagen deposition, and muscle fiber necrosis that were consistent with the WB condition (Velleman and Clark, 2015). Therefore, broilers were classified as either WB affected or unaffected based upon independent microscopic evaluations of the muscle samples by two trained laboratory personnel. If any 1 of the 4 positions were determined to have histological characteristics consistent with WB, the bird was considered to be positive for the WB condition. Therefore based on microscopic evaluation in total, 11 p. major muscle samples from Line A and 2 from Line B, were classified as positive for the WB

myopathy, while 9 p. major samples from Line A and 12 samples from line B were classified as unaffected. All 10 p. major samples isolated from Line C broilers remained classified as unaffected after microscopic examination.

Skeletal Muscle Morphology Scores. For each morphological parameter, a mean score was obtained from the four trained personnel for each sampling location. Morphology scores were considered to be ordinal multinomial data and therefore, the GENMOD procedure of SAS (2010, SAS Institute INC., Cary, NC) was used to model the categorical multinomial distribution. To reduce the number of comparisons, two statistical analyses were performed. The first analysis was completed to determine differences between broiler lines and WB status (affected or unaffected). The model included the main effects of line and WB status. Treatment means and standard error of the means (**SEM**) were determined with the least square means (**lsmeans**) statement and the diff option was used to separate interaction means. The second analysis was completed to determine the differences between the four different sampling regions within each broiler line. For this analysis, data were modeled as repeated measures from individual birds with the main effect of sampling location. Treatment means and SEM were determined with the lsmeans statement and the diff option was used to separate interaction means.

Fiber Diameter. Average fiber diameter analysis was completed in the MIXED procedure of SAS. As previously described, two statistical analyses were performed to determine differences between broiler lines with or without WB and differences between sampling locations. For the first analysis the model included the main effects of line and WB status. Treatment means and SEM were determined with the lsmeans statement and the pdiff option was used to separate interaction means. The second analysis was completed to determine differences

between sampling regions. As previously described, data were modeled as repeated measures with the main effect of sampling location. Treatment means were determined with the lsmeans statement and the pdiff option was used to separate interaction means.

The percentage of measured fibers with a diameter less than 10 µm or greater than 70 µm were calculated for each sampling region from every bird. The percentage of fibers within the given size constraints produced ordinal multinomial data and therefore, the GENMOD procedure of SAS was used to model the categorical multinomial distribution in the same manner as previously described for the morphological scores.

Gene Expression. Using the UNIVARIATE procedure of SAS, gene expression data were determined to be non-normal. Prior to analysis, the data were transformed with a natural log transformation. The MIXED procedure of SAS was then used in the same manner as described for average fiber diameter analysis, with an exception that 95% confidence limits were calculated with the lsmeans statement in substitute for SEM.

RESULTS

Pectoralis Major Muscle Morphological Structure

Figure 2 (A through H) contains representative images showing the p. major morphological structure of Line A in each of the regions sampled. In Line A, the AD and AV areas had extensive macrophage infiltration and fiber necrosis (Figure 2A and C). Necrotic regions were characterized by densely packed collagen fibrils in the perimysial space and more diffuse collagen in the endomysial space. In addition, myofiber cell size varied as giant fibers and small fibers were prevalent. In contrast, the unaffected p. major muscle from Line A at the AD and AV regions did not have infiltrating macrophages, fiber necrosis, or small fibers (Figure 2B and D), but did have giant, hypertrophic fibers. Unaffected p. major muscle from Line A at

the AD and AV areas also had minimal endomysial and perimysial spacing. The MV and PV regions in the unaffected p. major muscle from Line A (Figure 2F and H) were morphologically similar to the AD and AV regions, with the exception that endomysial spacing tended to increase towards the posterior region of the p. major muscle. In the WB affected Line A samples, the same observations that were noted in the AD and AV areas such as irregular fiber size, macrophage infiltration, and collagen deposition were also present within the MV sample but to a lesser degree (Figure 2E). In most cases the PV region of the WB affected Line A muscle (Figure 2G) contained few morphological observations consistent with the WB myopathy and therefore morphologically resembled the PV region of the unaffected p. major muscle.

Figure 3 contains representative photomicrographs showing the p. major morphological structure of Lines B and C in each of the four regions sampled. In contrast to Line A, the WB affected Line B p. major muscle at the AD region (Figure 3A) was morphologically similar to the AD region from unaffected WB p. major muscle (Figure 3B). The AV location of Line B WB affected muscle exhibited extensive fibrosis (Figure 3D). Similar to Line A, the AV location from Line B WB affected muscle had extensive macrophage infiltration, fiber necrosis, and diffuse endomysial collagen deposition. However in contrast to Line A, this region did not possess the densely packed collagen fibers in the perimysial space. The MV location of Line B WB affected muscle also had a similar morphology as the AV region (Figure 3G), but to a lesser severity. The PV region of WB affected p. major muscle (Figure 3J) was morphologically similar to the WB unaffected muscle at the same area (Figure 3K). Line C did not contain any morphological features associated with the WB myopathy at any of the p. major muscle sampling areas (Figure 3C, F, I, and L).

Photomicrographs were also scored to statistically analyze the morphological differences between sampling locations throughout the p. major muscle of the three broiler lines. Macrophage infiltration, fiber necrosis, and endomysial connective tissue deposition was not different ($P \geq 0.14$) between the unaffected p. major muscle from Lines A, B or C (Table 2) at any location. Perimysial connective tissue deposition was increased ($P = 0.04$) in the AV region of Line A WB unaffected p. major muscle compared to Line C. Perimysial connective tissue infiltration was not different ($P \geq 0.12$) at any of the other locations (AD, MV, PV) for the unaffected p. major muscle across the three lines.

Macrophage infiltration was increased ($P \leq 0.02$) in Line A WB affected p. major muscle at all sampling locations compared to unaffected Line A muscle (Table 2). In Line B, macrophage infiltration was also increased ($P \leq 0.04$) at the AV and MV areas in WB affected p. major muscle compared to the unaffected muscle. However, macrophage infiltration was not different ($P \geq 0.24$) between WB affected and unaffected p. major muscle from Line B at the AD and PV regions. It should also be noted that the affected p. major muscle at the AD region had increased macrophage infiltration ($P < 0.01$) in Line A compared to Line B while there were no differences at any other location ($P \geq 0.52$). Within the WB affected p. major muscle from Line A, macrophage infiltration was highest at the AD and AV regions ($P \leq 0.02$), least at the PV region ($P \leq 0.01$), and intermediate at the MV region ($P \leq 0.02$). In Line B, the AV region of WB affected p. major muscle had the highest ($P \leq 0.01$) macrophage infiltration compared to all other locations.

Fiber necrosis was increased ($P \leq 0.01$) in WB affected AV and MV areas compared to unaffected muscle for both Lines A and B (Table 2). Fiber necrosis was also increased ($P \leq 0.01$) in Line A, WB affected AD regions compared to unaffected. However, for Line B, fiber necrosis

was not different ($P = 0.13$) between WB affected and unaffected muscles at the AD region. There was no difference ($P \geq 0.06$) in fiber necrosis in the PV region between affected and unaffected p. major muscles regardless of line. When comparing WB affected p. major muscle from Lines A and B, fiber necrosis was increased ($P = 0.03$) in the AD region of Line A compared to Line B. However, fiber necrosis was decreased ($P \leq 0.01$) in the AV region of Line A compared to Line B. Within the WB affected muscle from Line A, the PV region had the least amount of fiber necrosis ($P \leq 0.03$), the AD and AV region had the most ($P \leq 0.03$), and the MV region was intermediate ($P \leq 0.03$). In the WB affected muscle from Line B, the PV location also had the least amount of fiber necrosis ($P \leq 0.01$), the AV location had the most fiber necrosis ($P \leq 0.01$), and the MV and AD locations were intermediate ($P \leq 0.02$).

Endomysial connective tissue was increased ($P \leq 0.02$) in the AD, AV, and MV locations of Lines A and B WB affected p. major muscle compared to unaffected p. major muscle (Table 2). At the PV location, endomysial connective tissue was decreased ($P \leq 0.01$) in Line A WB affected muscle compared to unaffected. There was no difference ($P = 0.14$) in the endomysial connective tissue content of affected and unaffected p. major muscles at the PV location in Line B. Within Line A, WB affected p. major muscle, endomysial connective tissue was increased ($P \leq 0.04$) in the AD, AV, and MV locations compared to the PV location. In the WB affected muscle from Line B, the AV location had the most endomysial connective tissue ($P \leq 0.01$), the PV location had the least ($P \leq 0.01$), and the MV location was intermediate ($P \leq 0.01$).

For both Lines A and B, perimysial connective tissue was increased ($P \leq 0.01$) in WB affected p. major muscle compared to unaffected muscle at the AV and MV locations (Table 2). At the AD and PV locations, perimysial connective tissue was increased ($P < 0.01$) in Line A WB muscle compared to unaffected muscle. Perimysial connective tissue content in WB affected

muscle from Line B was not different ($P \geq 0.07$) from unaffected p. major muscle at the AD and PV regions. Within Line A, WB affected p. major muscle, perimysial connective tissue content was highest ($P \leq 0.05$) at the AD and AV locations and least ($P \leq 0.05$) at the MV and PD locations. The perimysial connective tissue content was not different ($P \geq 0.07$) at any of the four locations in WB affected p. major muscle from Line B.

Myofiber Diameter

Average myofiber diameter was narrower ($P \leq 0.01$) in unaffected p. major muscle from Line C compared to both unaffected p. major muscles from Lines A and B, and the WB affected muscle from Line A at all sampling locations (Table 3). The average myofiber diameter of unaffected p. major muscle from Line C and Line B WB affected muscle were not different ($P \geq 0.33$) at the AV, MV, and AD regions. However, at the PV location, the average myofiber diameter was narrower ($P = 0.03$) in Line C muscle compared to unaffected Line B muscle. There was also no difference ($P \geq 0.38$) between the average myofiber diameter from Lines A and B unaffected p. major muscles at any region. Within Line C, the average myofiber diameter was the narrowest at the PV location ($P \leq 0.01$) compared to the other sampling regions. Additionally in Line C, the average myofiber diameter was narrower in the AV region ($P = 0.03$) compared to the AD region.

The average myofiber diameter of WB affected p. major muscle from Line A at all locations were not significantly different ($P \geq 0.15$) compared to the unaffected muscle from the same line (Table 3). The myofiber diameter was narrower ($P \leq 0.03$) in WB affected p. major muscle from Line B compared to unaffected muscle at the AD, AV, and MV regions. There was no difference ($P = 0.41$) between average myofiber diameter at the PV location between WB affected and unaffected muscles from Line B. Within the WB affected p. major muscles from

Lines A and B, the average myofiber diameter was not different ($P \geq 0.33$) across all sampling regions.

An analysis was also conducted to determine the percentage of fibers with a diameter less than 10 µm or greater than 70 µm to further understand how the distribution of the fiber diameters are altered by the WB myopathy (Table 3). The percentage of fibers with a diameter less than 10 µm was increased ($P \leq 0.04$) in Line A WB affected p. major muscle at the AV and MV locations compared to unaffected muscle. There was no difference ($P \geq 0.12$) in the percentage of myofibers with a diameter less than 10 µm between the WB affected and unaffected muscles of Line A at the AD and PV locations. There was also no difference ($P \geq 0.18$) in the percentage of myofibers with a diameter less than 10 µm between Line B WB affected and unaffected p. major muscles at any location. However within WB affected muscle from Line B, the percentage of myofibers with a diameter less than 10 µm was increased ($P \leq 0.04$) at the AV location compared to the MV and PV locations.

The number of fibers with a diameter greater than 70 µm was increased ($P \leq 0.02$) in both WB affected and unaffected p. major muscle from Line A compared to Line C at all sampling locations (Table 3). In both Lines A and B, the percentage of myofibers with a diameter greater than 70 increased ($P \leq 0.03$) in the AD regions compared to the PV location, regardless of WB status.

MYOD1, Myogenin, Decorin, and IGF1R Expression

The expression of *MYOD1* and myogenin were measured in WB affected and unaffected p. major muscles at each sampling location (Table 4). The expression of *MYOD1* was not different ($P \geq 0.11$) in unaffected muscle from Line C compared to Lines A or B at any sampling location. Expression of *MYOD1* was also not different across the four sampling regions in

unaffected muscle from Lines A ($P \geq 0.19$) and B ($P \geq 0.06$). For Line C, *MYOD1* expression was highest ($P \leq 0.03$) at the MV location compared to the AD and AV location. Expression of *MYOD1* in WB affected Line A muscle was increased ($P \leq 0.04$) over 1.7 fold compared to Line A unaffected muscle at all sampling locations. There was no difference ($P \geq 0.14$) between *MYOD1* expression in the WB affected and unaffected muscles from Line B at any sampling region. Expression of *MYOD1* was also not different amongst sampling regions for either Lines A ($P \geq 0.16$) or B ($P \geq 0.25$) WB affected muscle.

Similar to *MYOD1*, there was no difference ($P \geq 0.41$) in myogenin expression between any of the unaffected Lines A, B, or C (Table 4) p. major muscle. Myogenin expression was not different ($P \geq 0.09$) across the sampling regions in Line C. In Line A unaffected p. major muscle, the PV region had increased ($P \leq 0.01$) myogenin expression compared to the AD region. Myogenin expression was increased ($P \leq 0.05$) in the PV region compared to the AD, AV, and MV regions in Line B unaffected muscle. In WB affected Line A muscle, myogenin expression was increased ($P \leq 0.04$) over 2.7 fold at each sampling region compared to unaffected muscle. In Line B, myogenin expression was over 2.3 fold greater ($P \leq 0.02$) in WB affected p. major muscle at the AD, AV, and MV regions compared to unaffected p. major muscle. There was no difference ($P = 0.09$) between WB affected and unaffected muscles from Line B at the PV location. In Line A WB affected muscle, myogenin expression was increased ($P = 0.02$) in the PV region compared to the MV region. There was no difference ($P \geq 0.18$) in myogenin expression between the four sampling regions of Line B WB affected muscle.

The expression of decorin and *IGF1R* were measured in WB affected and unaffected p. major muscles at each sampling location (Table 5). Decorin expression did not differ ($P \geq 0.33$) between unaffected p. major muscle from Lines A and C. Decorin expression was also not

different ($P = 0.57$) in unaffected Line B p. major muscle compared to Line C at the MV region. However, at the AD, AV and PV region, decorin expression was increased ($P \leq 0.04$) in Line B unaffected muscle compared to unaffected muscle from Lines A and C. Decorin expression was increased at all sampling regions in WB affected Line A muscle compared to unaffected muscle from Line A. At the anterior regions, decorin expression was increased ($P \leq 0.01$) over 5.5 fold in Line A WB affected p. major muscle compared to unaffected muscle from Line A. Whereas at the PV location, decorin expression was only increased ($P \leq 0.01$) 2.6 fold in WB affected Line A muscle compared to unaffected muscle from Line A. Likewise, decorin expression was increased ($P = 0.01$) 2.6 fold in WB affected muscle from Line B compared to unaffected muscle at the AV region. Decorin expression was not affected ($P \geq 0.25$) by WB status in Line B at any of the other regions sampled (AD, MV, or PV). There was no difference in decorin expression amongst the four sampling regions within affected muscle from either Lines A ($P \geq 0.21$) or B ($P \geq 0.17$).

Expression of *IGF1R* was not different ($P \geq 0.07$) in unaffected muscle from Line A compared to Line C at any sampling region (Table 5). However, *IGF1R* expression was increased ($P \leq 0.02$) at the AD, AV, and MV regions of Line B unaffected muscle compared to Line C. In Line A unaffected p. major muscle, *IGF1R* expression was decreased ($P = 0.01$) in the AV region compared to the PV region. Within Line B, *IGF1R* expression was decreased ($P \leq 0.01$) in the unaffected muscles at the AD and AV regions compared to the PV region. In Line C, *IGF1R* expression at the AD region was decreased ($P \leq 0.04$) compared to both the MV and PV regions. At the AD, AV, and MV regions of Line A muscle, *IGF1R* expression was increased ($P \leq 0.04$) in WB affected muscles compared to unaffected muscles from Line A. Whereas, *IGF1R* in Line B affected muscle was only increased ($P \leq 0.03$) in WB affected muscle at the AV

sampling region compared to the Line B unaffected muscle. Expression of *IGF1R* was not affected ($P \geq 0.22$) by sampling region in WB affected muscle from Line A. However in Line B, *IGF1R* expression was increased ($P = 0.01$) in the AV region of WB affected p. major muscle compared to the AD region.

DISCUSSION

Although both Lines A and B exhibited fibrosis and macrophage infiltration consistent with the WB myopathy, fibrotic changes throughout the p. major muscle were distinct between the two lines in terms of the extracellular distribution of collagen fibers surrounding the cells. In Line A, the features consistent with the WB myopathy such as macrophage infiltration, fiber necrosis, and endomysial and perimysial connective tissue deposition were greatest in both the AD and AV regions of the p. major muscle compared to the PV region. In Line B, the WB fibrotic morphology was primarily associated with the AV region and not the AD region. Line B WB affected p. major muscle had less perimysial connective tissue in the AD region compared to the AV and AD regions of Line A WB affected muscle. Similar to the findings in the current study, Velleman and Clark (2015) reported differences in the morphological structure of WB affected p. major muscle between the same lines used in the current study.

Effect of Myofiber Diameter on the Etiology of Wooden Breast

Selection for increased growth has increased p. major muscle fiber area (Remignon et al., 1995; Dransfield and Sosnicki, 1999) without altering fiber type composition of the p. major muscle (Remignon et al., 1995). The p. major muscle is predominantly comprised of fast-twitch anaerobic type IIB muscle fibers (Remignon et al., 1995). Glycogen is the principal energy substrate for type IIB myofibers and is metabolized into lactic acid. Capillaries provide nutrients and remove metabolic waste products including heat and lactic acid. Lactic acid is then recycled

in the liver, converted into glycogen and returned back to circulation to be utilized as an energy substrate in the Cori Cycle (Cori and Cori, 1929; Bangsbo et al., 1991). Capillaries are located in the endomysial and perimysial space between muscle fibers and muscle fiber bundles, respectively. The increase in myofiber size due to growth selection strategies is the direct result of satellite cell mediated muscle fiber hypertrophy (Prentis et al., 1984; Dransfield and Sosnicki, 1999; Scheuermann et al., 2004). As shown by Wilson et al. (1990) and Velleman et al. (2003a) increased myofiber diameter limits available endomysial and perimysial spacing between individual fibers and fiber bundles (Wilson et al., 1990; Velleman et al., 2003a). The greater fiber size decreases the available space for vascularization which has been shown to be reduced in the p. major muscle of fast growing broilers (Hoving-Bolink et al., 2000). Anaerobic metabolic capacity has also increased in growth-selected lines, resulting in greater lactic acid production (Yost et al., 2002). Because the p. major muscle is a predominantly anaerobic muscle with limited blood supply, a further reduction in circulation will lead to elevated lactic acid accumulation and a further reduction in pH. These changes in the p. major muscle may be associated with the necrosis and onset of breast muscle myopathies including WB.

The asymmetrical shape and spatial growth differences of the p. major muscle may also contribute to the differential onset of the WB myopathy within the p. major muscle. The average myofiber diameter in the AD region of non-affected p. major muscle was wider than average myofibers from other sampled regions (AV, MV, and PV) in all three genetic lines. This has likely contributed to the increased thickness of the p. major anterior region which has been positively correlated with breast meat yield (Guernec et al., 2003). Furthermore, differences in myofiber diameter between regions within the p. major muscle are likely to contribute to the spatial differences of the WB myopathy.

The average myofiber diameter was wider at all locations in both WB affected and unaffected muscle from Lines A and B compared to Line C. However, the average myofiber diameter does not account for differences in the distribution of myofiber size. For example, both small regenerating fibers and larger hypercontracted fibers have been observed in p. major muscle affected by the WB myopathy (Sihvo et al., 2013; Velleman and Clark, 2015). If both of these myofiber types are present in the same muscle and sampling location the overall average fiber diameter may not significantly change, but fiber diameter variation would increase. Therefore, the percentage of large fibers with a diameter larger than 70 µm and small fibers with a diameter less than 10 µm were quantified.

In the current study the percentage of large fibers was greatest in the AD region and lowest in the PV region of WB affected muscle from Line A. The large fibers in the AD region of the p. major muscle may partially explain why the WB myopathy is most severe in this region. However, in Line A there was no difference between the percentage of large fibers in the unaffected and WB affected muscles at any of the sampling regions. This would suggest that the etiology of the WB myopathy is not completely myofiber size or growth dependent. Bailey et al. (2015) supports this conclusion, as they reported that the WB myopathy had a low heritability and genetic correlation with both growth and breast yield and the authors identified a population of broilers with a high growth rate and low propensity to develop WB.

The low heritability observed by Bailey et al. (2015) indicates that non-genetic causes account for most of the variation in WB; to date this is the best evidence for the relative role of genetics and environment. Many environmental factors such as incubation conditions (Buys et al., 1998, Collin et al., 2007, Piestun et al., 2009; 2011, Janisch et al., 2015), hatch time (Buys et al., 1998; Powell et al., 2016a; 2016b), ambient temperature (Collin et al., 2007, Piestun et al.,

2011), nutrition (Powell et al., 2016a; 2016b), and breeder age (Ulmer-Franco et al., 2010) have all been shown to directly impact skeletal muscle growth. Other studies examining incubation conditions (Piestun et al., 2009), ambient environmental temperature (Halevy et al., 2001; Harding et al., 2015; Clark et al., 2016), and nutrition (Powell et al., 2013; 2014a; 2014b; 2016a; 2016b) have demonstrated that changes in muscle growth are due to altered satellite cell activity. For example, a short transient elevation in incubation temperature (3 to 12 h per day) sufficiently increases myoblast and satellite cell proliferation which in turn results in larger myofibers and increased breast yield at the time of processing (Piestun et al., 2009, 2011, 2013). Velleman et al. (2010; 2014), have also altered satellite cell activity by restricting nutrients immediately after hatch, which in turn resulted in greater myofiber necrosis and degeneration at the time of market.

Satellite cells are multipotent and can transdifferentiate into non-myogenic cellular lineages such as adipocytes (Asakura et al., 2001; Shefer et al., 2004; Rossi et al., 2010). The transdifferentiation of satellite cells to adipocytes may play a role in the accumulation of lipids identified in WB affected muscle (Soglia et al., 2015; Trocino et al., 2015). Immediate posthatch nutrient deficiencies (Velleman et al., 2010, 2014) and thermal stress (Halevy et al., 2001) inhibit satellite cells from differentiating into multinucleated myotubes. The suppression in differentiation has been postulated by Velleman et al. (2010, 2014) to increase the pool of proliferating satellite cells, as MyoD expression is elevated. The accumulation of satellite cells incapable of differentiation may increase the likelihood of satellite cells to enter an adipogenic lineage. Additionally, Harding et al. (2015) and Powell et al. (2014b) reported altered in vitro temperature or nutrient conditions increased the expression of adipogenic genes by p. major satellite cells. Further research is needed to understand not only how single environmental

stimuli impact satellite cell activity and cellular mechanisms that govern growth, but also how individual environmental stimuli interact with one another.

In Line A, the percentage of small fibers (diameter < 10 μm) was increased in WB affected p. major muscle compared to unaffected muscle. These small myofibers were likely fibers undergoing regeneration, as the expression of myogenic regulatory factors, *MYOD1* and myogenin, were also increased in the WB affected muscles compared to the unaffected muscles. Under normal conditions, regeneration is initiated by muscle damage which activates satellite cells. Upon activation, satellite cells express the transcription regulatory factors myogenic factor 5 (***MYF5***) and *MYOD1,* which stimulate proliferation (Rudnicki et al., 1993, Cornelison and Wold, 1997). Satellite cells then begin to express myogenin and myogenic regulatory factor 4 (***MRF4***) as they begin to terminally differentiate and exit the cell cycle (Hasty et al., 1993; Smith et al., 1994; Cornelison and Wold, 1997). As satellite cells differentiate, they fuse to form myotubes. Immature, regenerating myotubes are small and characterized by centrally located nuclei (Lash et al., 1957). During maturation, the myotube will differentiate into myofibers which undergo hypertrophic growth and myonuclei will localize to the periphery of the muscle fiber (Lash et al., 1957). In Line B, the percentage of small fibers and *MYOD1* expression in WB affected muscle was not different compared to unaffected muscle. Myogenin expression was increased in Line B WB affected muscle at the AV and MV locations compared to unaffected muscle. Interestingly, MYOD1 expression was also increased in unaffected Line B p. major muscle compared to unaffected Line A muscle. Further research is needed to determine how myogenic regulatory factors and satellite cell mediated regeneration change over time in muscle affected by the WB myopathy.

The regeneration process repairs damaged muscle fibers and produces new muscle fibers that are similar to those that were damaged. Therefore, as the regeneration process reaches completion, the mature myofiber should have the same morphological characteristics as the original myofiber. In the anterior region of WB affected muscle there were many small, presumably regenerating myofibers. The abundance of these small fibers suggests that the maturation of the regenerating myofibers was being inhibited. The abundance of small, regenerating fibers in WB affected muscle is consistent with previous studies of the WB myopathy (Sihvo et al., 2013; Velleman and Clark, 2015). Furthermore, Velleman and Clark (2015) also reported elevated myostatin and transforming growth factor-β (***TGF-β***) expression within WB affected muscle compared to unaffected muscle in the same genetic lines. Both myostatin and *TGF-β* inhibit myofiber regeneration by repressing the proliferation and differentiation of satellite cells (Massagué et al, 1986; Amthor et al., 2002; McCroskery et al., 2003). The elevation in myostatin and *TGF-β* expression (Velleman and Clark; 2015) suggests an inhibitory mechanism blocking the repair and regeneration of WB damaged muscle fibers.

Myofiber regeneration is not only regulated by growth factors, but also the environment or niche surrounding the satellite cells. Kuang et al. (2008) described the satellite cell niche to include, but not limited to, the host myofiber, basal lamina, extracellular matrix, and microvasculature cells. The niche environment is required to initiate satellite cell activation either by paracrine signals or direct cell-to-cell contact. The importance of the niche environment is shown by approximately 80% of the satellite cells being located within 5 μm of capillaries (Christov et al., 2007). Additionally, angiogenesis and myofiber regeneration are codependent processes that are coordinated and occur simultaneously (Rhoads et al., 2009). It is not surprising that satellite cell mediated regeneration is dependent upon the close proximity to perivascular

cells (Rhoads et al., 2009). However, large muscle fibers can reduce available connective tissue space (Wilson et al., 1990; Velleman et al., 2003b), which will limit the amount of vascularization (Hoving-Bolink et al., 2000). It is therefore reasonable to hypothesize that the presence of large hypercontracted myofibers may contribute to both necrosis due to retained lactic acid, and inhibition of satellite cell mediated repair and regeneration.

Decorin Mediated Cell Signaling and Posttranslational Protein Modifications

Decorin is an extracellular small leucine-rich repeat proteoglycan that has multiple physiological roles including collagen crosslink formation (Weber et al., 1996; Danielson et al., 1997), TGF-β and myostatin sequestration (Schönherr et al., 1998; Riquelme et al., 2001; Brandan et al., 2008), and directly regulates cellular growth by binding to cellular receptors including IGF1R (Schönherr et al., 2005; Brandan et al., 2008; Fiedler et al., 2008, Iozzo et al., 2011). Decorin can either inhibit or promote cellular growth depending on its expression and receptor it interacts with (Li et al., 2008; Kishioka et al., 2008; Kanzleiter et al., 2014; Zeng et al., 2014). Decorin is comprised of ten leucine-rich repeats within the central domain that contain at least one high affinity binding site for fibrillar collagen (Weber et al., 1996). The decorin fibrillar collagen binding site facilitates proper collagen alignment and regulates collagen crosslinking (Danielson et al., 1997). The resulting mature, hydroxylsylpyridinoline (**HP**) trivalent crosslink is non-reducible. The WB affected p. major muscle from Line A had elevated decorin expression and a tight parallel organization of perimysial collagen fibrils, suggesting a high degree of collagen crosslinking (Velleman et al., 1996, 1997). The high levels of HP crosslinking will likely result in the rigid palpation of the p. major muscle associated with the WB myopathy. Despite the differences in the spatial severity of the WB morphology in Line A, decorin expression was not affected by sampling location. The increased decorin expression

throughout WB affected muscle may be the result of increased decorin expression prior to the onset of WB in the PV region which had minimal WB associated morphology. In Line B, however decorin expression was increased in the WB affected samples only at the AV region. Despite the increased decorin expression, the collagen fibril structure was diffuse and not in a tight parallel fibrils in the perimysium. In support of these observations, Velleman and Clark (2015) also reported differences in decorin expression between WB affected and unaffected muscles in the same genetic lines and similar differences in collagen fibril organization between Lines A and B.

Decorin can also interact with pro-myogenic growth factors. Insulin-like growth factor 1 (***IGF1***) promotes muscle growth and muscle regeneration by stimulating both satellite cell proliferation and differentiation (Kocamis et al., 2001). In endothelial cells, decorin can stimulate IGF1R phosphorylation and thereby evoke downstream growth stimulatory signaling pathways, analogous to IGF1 (Fiedler et al., 2008). However, in cancer cells decorin has been shown to antagonize IGF1R by preventing IGF1 activation (Iozzo et al., 2011). Regardless of the opposing decorin effects on different cell types, IGF1R plays a critical role in regulating cellular growth. Expression of IGF1R was increased in regions of the p. major muscle most severely affected by WB in both Lines A and B; whereas in regions minimally affected by WB, IGF1R expression was not different between WB affected and unaffected muscle. Taken together, these results strongly support a direct role for decorin in the WB myopathy. The potential involvement of decorin and its interaction and regulation of IGF1R expression in WB affected muscle needs to be further elucidated.

Summary

The present study demonstrated that the WB morphological characteristics such as fiber necrosis, macrophage infiltration, and connective tissue deposition were not uniform throughout the p. major muscle. The distribution of small muscle fibers and expression of myogenic regulatory factors was also not uniform throughout the p. major muscle. Additionally, decorin expression was increased in WB affected muscle compared to unaffected muscle from Line A. Interestingly, in Line A decorin expression was increased at all sampling locations in the p. major muscle despite the differences in fibrosis at different locations in the p. major muscle. In contrast, decorin expression in Line B, was increased only at the AV region of WB affected p. major muscle. Further research is needed to determine if differences in decorin expression across broiler lines mediate the phenotypes associated with WB in the two broiler lines.

ACKNOWLEDGEMENTS

The authors would like to thank Ms. Cynthia S. Coy and Dr. Rachel L. Harding for technical and editorial assistance.

REFERENCES

Amthor, H., R. Huang, I. McKinnell, B. Christ, R. Kambadur, M. Sharma, and K. Patel. 2002. The regulation and activation of myostatin as a negative regulator of muscle development during avian embryogenesis. Dev. Biol. 251:241-257.

Asakura A., M. Komaki, and M.A. Rudnicki. 2001. Muscle satellite cells are multipotential stem cells that exhibit myogenic, osteogenic, and adipogenic differentiation. Differentiation 68:245-253.

Bailey R. A., K. A. Watson, S. F. Bilgili, and S. Avendano. 2015. The genetic basis of pectoralis major myopathies in modern broiler chicken lines. Poult. Sci. 94:2870-2879

Bangsbo, J., P. D. Gollnick, T. E. Grahm, and B. Saltin. 1991. Substrates for muscle glycogen synthesis in recovery from intense exercise in man. J. Physiol. 434:423-440.

Brandan, E., C. Cabello-Verrugio, and C. Vial. 2008. Novel regulatory mechanisms for the proteoglycans decorin and biglycan during muscle formation and muscular dystrophy. Matrix Biol. 27:700-708.

Berri, C., E. L. Bihan-Duval, M. Debut, V. Santé-Lhoutellier, E. Baéza, V. Gigaud, Y. Jégo, and M. J. Duclos. 2007. Consequence of muscle hypertrophy on characteristics of pectoralis major muscle and breast meat quality of broiler chickens. J. Anim. Sci. 85: 2005-2011.

Buys, N., E. Dewil, E. Gonzales, and E. Decuypere. 1998. Different CO2 levels during incubation interact with hatching time and ascites susceptibility in two broiler lines selected for different growth rate. Avian. Pathol. 27:605-612.

Christov, C., F. Chrétien, R. Abou-Khalil, G. Bassez, G. Vallet, F.-GJ. Authier, Y. Bassaglia, V. Shinin, S. Tajbakhsh, B. Chazaud, and R. K. Gherardi. 2007. Muscle satellite cells and endothelial cells: Close neighbors and privileged partners. Mol. Biol. Cell. 18:1397-1409.

Clark, D. L., C. S. Coy, G. M, Strasburg, K. M. Reed, and S. G. Velleman. 2016. Temperature effect on proliferation and differentiation of satellite cells from turkeys with different growth rates. Poult. Sci. In Press. DOI: 10.3382/ps/pev437.

Cori, C. F and G. T. Cori. 1929. Glycogen formation in the liver from d- and l- lactic acid. J. Biol. Chem. 81:389-403.

Cornelison, D. D. W. and B. J. Wold. 1997. Single-cell analysis of regulatory gene expression in quiescent and activated mouse skeletal muscle in satellite cells. Dev. Biol. 191:270-283.

Collin A., C. Berri, S. Tesseraud, F. E. Requena Rodón, S. Skiba-Cassy, S. Crochet, M. J. Duclos, N. Rideau, K. Tona, J. Buyse, V. Bruggeman, E.Decuypere, M. Picard, and S. Yahav. 2007. Effects of thermal manipulation during early and late embryogenesis on thermotolerance and breast muscle characteristics in broiler chickens. Poult. Sci. 86:795-800.

Collins, K. E., B. H. Kiepper, C. W. Ritz, B. L. McLendon, and J. L. Wilson. 2014. Growth, livability, feed consumption, and carcass composition of the Athens Canadian Random Bred 1955 meat-type chicken versus the 2012 high-yielding Cobb 500 broiler. Poult. Sci. 93:2953-2962.

Danielson K. G., H. Baribault, D. F. Holmes, H. Graham, K. E. Kadler, R. V. Iozzo. 1997. Targeted disruption of decorin leads to abnormal collagen fibril morphology and skin fragility. J. Cell Biol. 136:729-743.

Dransfield E. and A. A. Sosnicki. 1999. Relationship between muscle growth and poultry meat quality. Poult. Sci. 78:743-746.

Fielder, L. R. , E. Schönherr, R. Waddington, S. Niland, D. G. Seidler, D. Aeschlimann, and J. A. Elbe. 2008. Decorin regulates endothelial cell motility on collagen I through activation

of Insulin-like growth factor 1 receptor and modulation of α2β1 integrin activity. J. Biol. Chem. 283:17406-17415.

Guernec, A., C. Berri, B. Chevalier, N. Wacrenier-Cere, E. L. Bihan-Duval, and M. J. Duclos. 2003. Muscle development, insulin-like growth factor-I and Myostatin mRNA levels in chickens selected for increased breast muscle yield. Growth Horm. IGF Res. 13:8-18.

Halevy, O., A. Krispin, Y. Leshem, J. P. McMurty, and S. Yahav. 2001. Early-age heat exposure affects skeletal muscle satellite cell proliferation and differentiation in chicks. Am. J. Physiol-Reg. I. Comp. Physiol. 281:R302-R309.

Harding R. L., D. L. Clark, O. Halevy, C. S. Coy, S. Yahav, and S. G. Velleman. 2015. The effect of temperature on apoptosis and adipogenesis on skeletal muscle satellite cells derived from different muscle types. Physiol. Rep. 3:e12539.

Hasty, P., A. Bradley, J. H. Morris, D. G. Edmondson, J. M. Venuti, E. N. Olson, and W. H. Klein. 1993. Muscle deficiency and neonatal death in mice with a targeted mutation in the myogenin gene. Nature. 364:501-506.

Hoving-Bolink A. H., R. W. Kranen, R. E. Klont, C. L. M. Gerritsen, and K. H. de Greef. 2000. Fibre area and capillary supply in broiler breast muscle in relation to productivity and ascites. Meat Sci. 56:397-402.

Iozzo, R. V., S. Buraschi, M. Genua, S.-Q. Xu, C. C. Solomides, S. C. Peiper, L. G. Gomella, R. T. Owens, and A. Morrione. 2011. Decorin antagonizes IGF receptor I (IGF-IR) function by interfering with IGF-IR activity and attenuating downstream signaling. J. Biol. Chem. 283:17406-17415.

Jarrold, B. B., W. L. Bacon, and S. G. Velleman. 1999. Expression and localization of the proteoglycan decorin during the progression of cholesterol induced atherosclerosis in

Japanese quail: implications for interaction with collagen type I and lipoproteins. Atherosclerosis 146: 299-308.

Janisch, S., A. R. Sharifi, M. Wicke, and C. Krischek. 2015. Changing the incubation temperature during myogenesis influences the weight performance and meat quality of male and female broilers. Poult. Sci. 94:2581-2588.

Kanzleiter, T., M. Rath, S. W. Görgens, J. Jensen, D. S. Tangen, A. J. Kolnes, K. J. Kolnes, S. Lee, J. Eckel, A. Schürmann, and K. Eckardt. 2014. The myokine decorin is regulated by contraction and involved in muscle hypertrophy. Biochem. Biophys. Res. Commun. 450:1089-1094.

Kijowski, J. and M. Konstanczak. 2009. Deep pectoral myopathy in broiler chickens. Bull. Vet. Inst. Pulawy. 53:487-491.

Kindlein L., L. M. Lorscheitter, T. Z. Ferreira, R. Sesterhenn, S. Rauber, P. Soster, and S. Vieira. 2015. Occurrence of wooden breast in broilers breast fillets in different weights. Poult. Sci. 94 (E-Suppl. 1):160.(Abstr.).

Kishioka, Y., M. Thomas, J. Wakamatsu, A. Hattori, M. Sharma, R. Kambadur, and T. Nishimura. 2008. Decorin enhances the proliferation and differentiation of myogenic cells through suppressing myostatin activity. J. Cell. Physiol. 215:856-867.

Kocamis, H., D. C. McFarland, and J. Killefer. 2001. Temporal expression of growth factor genes during myogenesis of satellite cells derived from the biceps femoris and pectoralis major muscles of the chicken. J. Cell. Physiol. 186:146-152.

Kuang, S., M. A. Gillespie, and M. A. Rudnicki. 2008. Niche regulation of muscle satellite cell self-renewal and differentiation. Cell Stem Cell 2:22-31.

Kuttappan, V. A., V. B. Brewer, J. K. Apple, P. W. Waldroup, and C. M. Owens. 2012. Influence of growth rate on the occurrence of white striping in broiler breast fillets. Poult. Sci. 91:2677-2685.

Kuttappan,, V. A., H. L. Shivaprasad, D. P. Shaw, B. A. Valentine, B. M. Hargis, F. D. Clark, S. R. McKee, and C. M. Owens. 2013. Pathological changes associated with white striping in broiler breast muscles. Poult. Sci. 92: 331-338.

Lash, J. W., H. Holtzer, and H. Swift. 1957. Regeneration of mature skeletal muscle. Anat. Rec. 127:679-697.

Li, Z. B., H. D. Kollias, and K. R. Wagner. 2008. Myostatin directly regulates skeletal muscle fibrosis. J. Biol. Chem. 283:19371-19378.

Liu, C., D. C. McFarland, K. E. Nestor, and S. G. Velleman. 2006. Differential expression of membrane-associated heparan sulfate proteoglycans in the skeletal muscle of turkeys with different growth rates. Poult. Sci. 85:422-428.

Luque, E., J. Peña, P. Martin, I. Jimena, and R. Vaamonde. 1995. Capillary supply during development of individual regenerating muscle fibers. Anat. Histol. Embryol. 24:87-89.

Macrae, V. E., M. Mahon, S. Gilpin, D. A. Sandercock, and M. A Mitchell. 2006. Skeletal muscle fibre growth and growth associated myopathy in the domestic chicken (*Gallus domesticus*). Br. Poult. Sci. 47:264-272.

Massagué, J., S. Cheifetz, T. Endo, and B. Nadal-Ginard. 1986. Type beta transforming growth factor is an inhibitor of myogenic differentiation. Proc. Natl. Acad. Sci. USA 83:8206-8210.

Mauro, A. 1961. Satellite cell of skeletal muscle fibers. J. Biophys. Biochem. Cytol. 9:493-495.

Mazzoni, M., M. Petracci, A. Meluzzi, C. Cavani, P. Clavenzani, and F. Sirri. 2015. Relationship between pectoralis major muscle histology and quality traits of chicken meat. Poult. Sci. 94:123-130.

McCroskery, S., M. Thomas, L. Maxwell, M. Sharma, and R. Kambadur. 2003. Myostatin negatively regulates satellite cell activation and self-renewal. J. Cell Biol. 162:1135-1147.

Moss, F. P., and C. P. LeBlond. 1971. Satellite cells are the source of nuclei in muscles of growing rats. Anat. Rec. 170:421-435.

Mudalal, S., M. Lorenzi, F. Soglia, C. Oavani, and M. Petracci. 2015. Implications of white striping and wooden breast abnormalities on quality traits of raw and marinated chicken meat. Animal 9:728-734.

OECD-FAO. 2015. OECD-FAO Agricultural Outlook 2015, OECD Publishing, Paris. doi: 10.1787/agr_outlook-2105-en.

Petracci, M. and C. Cavani. 2012. Muscle growth and poultry meat quality issues. Nutrients 4:1-12.

Petracci, M., S. Mudalal, A. Bonfiglio, and C. Cavani. 2013. Occurrence of white striping under commercial conditions and its impact on breast meat quality in broiler chickens. Poult. Sci. 92:1670-1675.

Petracci, M., S. Mudalal, F. Soglia, and C. Cavani. 2015. Meat quality in fast-growing broiler chickens. Worlds Poult. Sci. J. 71:363-374.

Piestun, Y., M. Harel, M. Garak, S. Yahav, and O. Halevy. 2009. Thermal manipulations in late-term chick embryos have immediate and longer term effects on myoblast proliferation and skeletal muscle hypertrophy. J. Appl. Physiol. 106:233-240.

Piestun, Y., O. Halevy, D. Shinder, M. Ruzal, S. Druyan, and S. Yahav. 2011. Thermal manipulations during broiler embryogenesis improves post-hatch performance under hot conditions. J. Therm. Biol. 36:469-474.

Powell, D. J., D. C. McFarland, A. J. Cowieson, W. I. Muir, and S. G. Velleman. 2013. The effect of nutritional status on myogenic gene expression of satellite cell proliferation and differentiation. Poult. Sci. 92:2163-2173

Powell, D. J., D. C. McFarland, A. J. Cowieson, W. I. Muir, and S. G. Velleman. 2014a. The effect of nutritional status on myogenic gene expression of satellite cells derived from different muscle types. Poult. Sci. 93:2278-2288.

Powell, D. J., D. C. McFarland, A. J. Cowieson, W. I. Muir, and S. G. Velleman. 2014b. The effect of nutritional status and muscle fiber type on myogenic satellite cell fate and apoptosis. Poult. Sci. 93:163-173.

Powell, D. J., S. G. Velleman, A. J. Cowieson, M. Singh, and W. I. Muir. 2016a. Influence of chick hatch time and access to feed on broiler muscle development. Poult. Sci. In Press.

Powell, D. J., S. G. Velleman, A. J. Cowieson, M. Singh, and W. I. Muir. 2016b. Influence of chick hatch time and access to feed on intramuscular adipose tissue deposition in broilers. Poult. Sci. In Press.

Prentis, P. F., R. K. Penney, and G. Goldspink. 1984. Possible use of an indicator muscle in future breeding experiments in domestic fowl. Br. Poult. Sci. 25:33-41.

Remignon, H., M. –F. Gardahaut, G. Marche, and F. –H. Ricard. 1995. Selection for rapid growth increases the size of fibers without changing their typing in chickens. J. Muscle. Res. Cell Motil. 16:95-102.

Rhoades, R. P., K. L. Flann, T. R. Cardinal, C. R. Rathbone, X. Liu, and R. E. Allen. 2013. Satellite cells isolated from aged or dystrophic muscle exhibit a reduced capacity to promote angiogenesis *in vitro.* Biochem. Biophys. Res. Commun. 440:399-404.

Rhoades, R. P., R. M. Johnson, C. R. Rathbone, X. Liu, C. Temm-Grove, S. M. Sheehan, J. B. Hoying, and R. E. Allen. 2009. Satellite cell-mediated angiogenesis in vitro coincides with a functional hypoxia-inducible factor pathway. Am. J. Physiol. 296:C1321-C1328.

Richardson, J.A., J. Burgener, R.W. Winterfield, and A.S. Dhillon. 1980. Deep pectoral myopathy in seven-week-old chickens. Avian Dis. 24:1054-1059.

Riquelme, C., J. Larraín, E. Schönherr, J. P. Henriquez, H. Kresse, and E. Brandan. 2001. Antisense inhibition of decorin expression in myoblasts decreases cell responsiveness to transforming growth factor β and accelerates skeletal muscle differentiation. J. Biol. Chem. 276:3589-3596.

Rossi, C.A., M. Pozzobon, A. Ditadi, K. Archacka, A. Gastaldello, M. Sanna, C. Franzin, A. Malerba, G. Milan, M. Cananzi, S. Schiaffino, M. Campanella, R. Vettor, and P.D. Coppi. 2010. Clonal characterization of rat muscle satellite cells: proliferation, metabolism, and differentiation define an intrinsic heterogeneity. PLoS One. 5:e8523.

Rudnicki, M. A., P. N. Schnegelsberg, R. H. Stead, T. Braun, H. H. Arnold, and R. Jaenisch. 1993. MyoD or Myf-5 is required for the formation of skeletal muscle. Cell. 75:1351-1359.

Sandercock, D. A., R. R. Hunter, G. R. Nute, M. A. Mitchell, and P. M. Hocking. 2001. Acute heat stress-induced alterations in blood acid-base status and skeletal muscle membrane integrity in broiler chickens at two ages: Implications for meat quality. Poult. Sci. 80:418-425.

Scheuermann, G. N., S. F. Bilgili, S. Tuzun, and D. R. Mulvaney. 2004. Comparison of chicken genotypes: Myofiber number in pectoralis muscle and myostatin ontogeny. Poult. Sci. 83:1404-1412.

Schönherr, E., M. Broszat, E. Brandan, P. Bruckner, and H. Kresse. 1998. Decorin core protein fragment Leu155-Val260 interacts with TGF-beta but does not compete for decorin binding to type I collagen. Arch. Biochem. Biophys. 355:241-248.

Schönherr, E., C. Sunderkötter, R. V. Iozzo, and L. Schaefer. 2005. Decorin, a novel player in the insulin-like growth factor system. J. Biol. Chem. 280:15767-15772.

Shefer G., M. Wleklinski-Lee, and Z. Yablonka-Reuveni. 2004. Skeletal muscle satellite cells can spontaneously enter an alternative mesenchymal pathway. J. Cell Sci. 117:5393-5404.

Sihvo, H. K., K. Immonen, and E. Puolanne. 2013. Myodegeneration with fibrosis and regeneration in the pectoralis major muscle of broilers. Vet. Pathol. 51:619-623.

Siller, W.G. 1985. Deep pectoral myopathy: A penalty of successful selection for muscle growth. Poult. Sci. 64:1591-1595.

Smith, J.H. 1963. Relation of body size to muscle cell size and number in the chicken. Poult. Sci. 42:283-290.

Smith, C. K., II, M. J. Janney, and R. E. Allen. 1994. Temporal expression of myogenic regulatory genes during activation, proliferation, and differentiation of rat skeletal muscle satellite cells. J. Cell. Physiol. 159:379-385.

Soglia, F., S. Mudalal, E. Babini, M. D. Nunzio, M. Mazzoni, F. Sirri, C. Cavani, and M. Petracci. 2015. Histology, composition, and quality traits of chicken *Pectoralis major*

muscle affected by wooden breast abnormality. Poult. Sci. In Press DOI:10.3382/ps/pev353.

Stockdale, F. E. and H. Holtzer. 1961. DNA synthesis and myogenesis. Exp. Cell Res. 24:508-520.

Trocino, A., A. Piccirillo, M. Birolo, G. Radaelli, D. Bertotto, E. Filiou, M. Petracci, and G. Xiccato. 2015. Effect of genotype, gender and feed restriction on growth, meat quality and the occurrence of white striping and wooden breast in broiler chickens. 94:2996-3004.

Ulmer-Franco, A. M., G. M. Fasenko, and E. E. O'Dea Christopher. 2010. Hatching egg characteristics, chick quality, and broiler performance at 2 breeder flock ages and from 3 egg weights. Poult. Sci. 89:2735-2742.

Van Laack, R.L.J.M., C.-H. Liu, M. O. Smith, and H. D. Loveday. 2000. Characteristics of pale, soft, exudative broiler breast meat. Poult. Sci. 79:1057-1061.

Velleman, S. G. 2015. Relationship of skeletal muscle development and growth to breast muscle myopathies: A Review. Avian Dis. 59:525-531.

Velleman, S. G., J. W. Anderson, C. S. Coy, and K. E. Nestor. 2003a. Effect of selection for growth rate on muscle damage during turkey breast muscle development. Poult. Sci. 82:1069-1074.

Velleman, S. G., C. S. Coy, J. W. Anderson, R. A. Patterson, and K. E. Nestor. 2003b. Effect of selection for growth rate and inheritance on posthatch muscle development in turkeys. Poult. Sci. 82:1365-1372.

Velleman S.G., C.S. Coy, and D.A. Emmerson. 2014. Effect of the timing of posthatch feed restriction on the deposition of fat during broiler breast muscle development. Poult. Sci. 93:2622-2627.

Velleman, S. G. and D. L. Clark. 2015. Histopathologic and myogenic gene expression changes associated with wooden breast in broiler breast muscles. Avian Dis. 59:410-418.

Velleman, S.G., D.C. McFarland, Z. Li, N.H. Ferrin, R. Whitmoyer, and J.E. Dennis. 1997. Alterations in sarcomere structure, collagen organization, mitochondrial activity, and protein metabolism, in the avian low score normal muscle weakness. Dev. Growth Differ. 39:563-570.

Velleman S. G., K. E. Nestor, C. S. Coy, I. Harford, and N. B. Anthony. 2010. Effect of posthatch feed restriction on broiler breast muscle development and muscle transcriptional regulatory factor gene and heparan sulfate proteoglycan expression. Int. J. Poult. Sci. 9:417-425.

Velleman, S. G., J. D. Yeager, H. Krider, D. A. Carrino, S. D. Zimmerman, and R. J. McCormick. 1996. The avian low score normal muscle weakness alters decorin expression and collagen crosslinking. Connect. Tissue Res. 34:33-39.

Weber, I. T., R. W. Harrison, and R. V. Iozzo. 1996. Model structure of decorin and implications for collagen fibrillogenesis. J. Biol. Chem. 271:31767-31770.

Wilson, B.W., P.S. Nieberg, and R.J. Buhr. 1990. Turkey muscle growth and focal myopathy. Poult. Sci. 69:1553-1562.

Woelfel, R. L., C. M. Owens, E. M. Hirschler, R. Martinez-Dawson, and A. R. Sams. 2002. The characterization and incidence of pale, soft, and exudative broiler meat in a commercial processing plant. Poult. Sci.81:579-584.

Yost, J. K., P. B. Kenney, S. D. Slider, R. W. Russell, and J. Killefer. 2002. Influence of selection for breast muscle mass on myosin isoform composition and metabolism of deep pectoralis muscles of male and female turkeys. Poult. Sci. 81:911-917.

Zeng, Q. J., L. N. Wang, G. Shu, S. B. Wang, X. T. Zhu, P. Gao, Q. Y. Xi, Y. L. Zhang, Z. Q. Zhang, and Q. Y. Jiang. 2014. Decorin-induced proliferation of avian myoblasts involves the myostatin/Smad signaling pathway. Poult. Sci. 93:138-146.

Zotte, A. D., M. Cecchinato, A. Quartesan, J. Bradanovic, G. Tasoniero, and E. Puolanne. 2014. How does “wooden breast” myodegeneration affect poultry meat quality. Arch. Latinoam. Prod. An. 22: 476-479.

Table 1. Primer sequences for real-time quantitative polymerase chain reaction.

Primer	Sequence	Coding Region	Product Size (bp[5])	GenBank Accession Number
MYOD1[1]	5'-GAC GGC ATG ATG GAG TAC AG-3'	553-572	201	AY641567.1
	5'-AGC TTC AGC TGG AGG CAG TA-3'	734-753		
MYOG[2]	5'-CCT TTC CCA CTC CTC TCC AAA-3'	813-833	175	AY560111.3
	5'-GAC CTT GGT CGA AGA GCA ACT-3'	967-987		
Decorin	5'-AAGGTTCTGCCTGGAGTTGA-3'	102-121	254	NM_001030747.2
	5'-TTGGCACTCTTTCCAGACCT-3'	336-355		
IGF1R[3]	5’-ACCTTGTTGTGCTTGTCCCA-3’	2233-2252	219	NM_205032.1
	5’-TCTGCGTCAGAAGCATTGGT-3’	2432-2451		
GAPDH[4]	5'-GAG GGT AGT GAA GGC TGC TG-3'	504-523	200	U94327.1
	5'-CCA CAA CAC GGT TGC TGT AT-3'	684-703		

[1]*MYOD1* = Myogenic Determination Factor 1
[2]*MYOG* = Myogenin
[3]*IGF1R* = Insulin-like Growth Factor Type 1 Receptor
[4]*GAPDH* = Glyceraldehyde-3-phosphate dehydrogenase
[5]bp = Base pairs of DNA

Table 2. Histological morphology scores at four different locations within the pectoralis major muscle of three different genetic lines affected or unaffected by the wooden breast (WB) myopathy.[1]

	Line A		Line B		Line C
Location	WB Affected	Unaffected	WB Affected	Unaffected	Unaffected
Macrophage Infiltration					
AD[2]	$2.55 \pm 0.26^{c,x}$	$4.65 \pm 0.32^{a,z}$	$3.66 \pm 0.52^{b,z}$	$4.12 \pm 0.23^{ab,z}$	$4.53 \pm 0.23^{a,z}$
AV[2]	$2.48 \pm 0.22^{b,x}$	$4.25 \pm 0.27^{a,y}$	$2.69 \pm 0.35^{b,y}$	$4.20 \pm 0.19^{a,z}$	$4.32 \pm 0.19^{a,z}$
MV[2]	$3.12 \pm 0.24^{b,y}$	$4.33 \pm 0.30^{a,yz}$	$3.22 \pm 0.34^{b,z}$	$4.04 \pm 0.21^{a,z}$	$4.38 \pm 0.21^{a,z}$
PV[2]	$3.67 \pm 0.13^{b,z}$	$4.28 \pm 0.22^{a,y}$	$3.82 \pm 0.39^{ab,z}$	$4.15 \pm 0.15^{a,z}$	$4.28 \pm 0.15^{a,z}$
Fiber Necrosis					
AD	$2.48 \pm 0.20^{c,x}$	$4.05 \pm 0.26^{a,z}$	$3.19 \pm 0.31^{b,yz}$	$3.70 \pm 0.18^{ab,z}$	$3.94 \pm 0.18^{a,z}$
AV	$3.13 \pm 0.22^{b,y}$	$3.90 \pm 0.27^{a,y}$	$2.24 \pm 0.30^{c,x}$	$3.85 \pm 0.19^{a,z}$	$3.93 \pm 0.19^{a,z}$
MV	$3.20 \pm 0.14^{b,yz}$	$3.88 \pm 0.24^{a,yz}$	$3.00 \pm 0.39^{b,y}$	$3.71 \pm 0.17^{a,z}$	$3.83 \pm 0.19^{a,z}$
PV	$3.48 \pm 0.17^{a,z}$	$4.00 \pm 0.24^{a,yz}$	$3.57 \pm 0.27^{a,z}$	$3.89 \pm 0.19^{a,z}$	$3.89 \pm 0.17^{a,z}$
Endomysial Connective Tissue					
AD	$2.35 \pm 0.29^{c,y}$	$4.77 \pm 0.35^{a,yz}$	$3.38 \pm 0.64^{b,yz}$	$4.58 \pm 0.25^{a,z}$	$4.58 \pm 0.25^{a,z}$
AV	$2.37 \pm 0.26^{b,y}$	$4.63 \pm 0.30^{a,z}$	$2.00 \pm 0.33^{b,x}$	$4.35 \pm 0.21^{a.yz}$	$4.30 \pm 0.21^{a,y}$
MV	$2.89 \pm 0.27^{b,y}$	$4.50 \pm 0.33^{a,y}$	$3.17 \pm 0.34^{b,y}$	$4.15 \pm 0.24^{a,yz}$	$4.38 \pm 0.23^{a,yz}$
PV	$3.39 \pm 0.25^{c,z}$	$4.63 \pm 0.26^{a,yz}$	$3.67 \pm 0.47^{bc,z}$	$4.17 \pm 0.19^{ab,y}$	$4.20 \pm 0.18^{ab,yz}$
Perimysial Connective Tissue					
AD	$2.31 \pm 0.26^{b,x}$	$4.20 \pm 0.32^{a,z}$	$3.66 \pm 0.52^{a,z}$	$3.93 \pm 0.23^{a,z}$	$4.24 \pm 0.23^{a,z}$
AV	$2.41 \pm 0.23^{d,xy}$	$3.55 \pm 0.28^{bc,y}$	$2.75 \pm 0.31^{cd,z}$	$3.88 \pm 0.20^{ab,z}$	$4.26 \pm 0.20^{a,z}$
MV	$2.89 \pm 0.16^{b,yz}$	$4.00 \pm 0.27^{a,yz}$	$3.04 \pm 0.30^{b,z}$	$3.94 \pm 0.19^{a,z}$	$4.00 \pm 0.19^{a,z}$
PV	$3.23 \pm 0.13^{c,z}$	$4.30 \pm 0.22^{a,z}$	$3.34 \pm 0.35^{bc,z}$	$3.88 \pm 0.17^{ab,z}$	$4.09 \pm 0.15^{a,z}$

[1]Scores ranged from 1 to 5, with 1 being extensive macrophage infiltration, fiber necrosis, endomysial connective tissue deposition, or perimysial connective tissue deposition; a score of 5 would imply the muscle was morphologically normal.

[2]AD = Anteriodorsal; AV = Anterioventral; MV = Middle Ventral; PV = Posterioventral.

[a-d]Means ± SEM within a row (sampling region) without a common letter are significantly different ($P < 0.05$)

[x-z]Means ± SEM within a column (line/WB affection status) without a common letter are significantly different ($P<0.05$)

Table 3. Average fiber diameter and percentage of fibers with a diameter less than 10 μm or greater than 70 μm at four different locations within the pectoralis major muscle of three different genetic lines affected or unaffected by the wooden breast (WB) myopathy.

	Line A		Line B		Line C
Location	WB Affected	Unaffected	WB Affected	Unaffected	Unaffected
Average					
AD[1]	44.4 ± 1.6^{ab,z}	48.6 ± 2.7^{ab,z}	41.3 ± 3.0^{bc,z}	49.3 ± 1.9^{a,z}	37.8 ± 1.9^{c,z}
AV[1]	43.0 ± 1.6^{a,z}	47.7 ± 2.7^{a,z}	35.1 ± 3.1^{b,z}	44.7 ± 1.9^{a,y}	35.4 ± 1.9^{b,y}
MV[1]	43.9 ± 1.5^{a,z}	48.2 ± 2.7^{a,yz}	39.3 ± 3.0^{b,z}	47.4 ± 1.9^{a,yz}	37.2 ± 1.9^{b,yz}
PV[1]	42.7 ± 1.3^{a,z}	42.5 ± 2.2^{a,y}	38.2 ± 2.5^{a,z}	40.7 ± 1.6^{a,x}	31.5 ± 1.6^{b,x}
Percentage of cells less than 10 μm					
AD	2.22 ± 0.48^{a,z}	0.74 ± 0.83^{a,yz}	1.21 ± 0.93^{a,yz}	0.93 ± 0.59^{a,z}	1.38 ± 0.59^{a,y}
AV	3.07 ± 0.54^{a,z}	0.32 ± 0.94^{c,y}	3.17 ± 1.06^{ab,z}	1.50 ± 0.67^{abc,z}	1.25 ± 0.67^{bc,y}
MV	2.33 ± 0.56^{a,z}	0.00 ± 0.98^{b,y}	1.44 ± 1.09^{ab,y}	0.73 ± 0.69^{ab,z}	2.01 ± 0.69^{ab,yz}
PV	1.94 ± 0.45^{ab,z}	1.75 ± 0.79^{ab,z}	0.46 ± 0.88^{b,y}	1.47 ± 0.56^{ab,z}	2.83 ± 0.56^{a,z}
Percentage of cells greater than 70 μm					
AD	11.46 ± 1.99^{a,z}	10.34 ± 3.44^{a,z}	4.84 ± 3.85^{ab,z}	11.44 ± 2.44^{a,z}	0.64 ± 2.44^{b,yz}
AV	10.50 ± 1.93^{a,yz}	9.78 ± 3.34^{a,yz}	2.50 ± 3.74^{ab,x}	5.30 ± 2.36^{ab,y}	0.40 ± 2.36^{b,yz}
MV	9.13 ± 1.71^{a,yz}	11.29 ± 2.97^{a,yz}	4.30 ± 3.32^{ab,yz}	7.03 ± 2.09^{ab,yz}	1.53 ± 2.10^{b,z}
PV	6.96 ± 1.20^{a,y}	5.96 ± 2.07^{ab,y}	2.47 ± 2.32^{abc,xy}	1.72 ± 1.47^{bc,x}	0.00 ± 1.47^{c,y}

[1]AD = Anteriodorsal; AV = Anterioventral; MV = middle ventral; PV = Posterioventral.

$^{a-c}$Means ± SEM within a row (sampling region) without a common letter are significantly different (P< 0.05)

$^{x-z}$Means ± SEM within a column (line/WB affection status) without a common letter are significantly different (P<0.05)

Table 4. Myogenic determination factor 1 (*MYOD1*) and Myogenin expression at four different locations within the pectoralis major muscle of three different genetic lines affected or unaffected by the wooden breast (WB) myopathy.

	Line A		Line B		Line C
Location	WB Affected	Unaffected	WB Affected	Unaffected	Unaffected
MYOD1					
AD[1]	37.28^{a,z} (27.15-51.19)	15.82^{b,z} (9.13-27.4)	23.26^{ab,z} (12.58-42.98)	17.92^{b,z} (12.15-26.43)	17.74^{b,y} (12.03-26.16)
AV[1]	33.32^{a,z} (26.13-42.51)	12.30^{c,z} (8.07-18.75)	37.94^{a,z} (23.68-60.78)	25.02^{ab,z} (18.57-33.71)	17.87^{bc,y} (13.26-24.08)
MV[1]	29.48^{a,z} (22.36-38.86)	16.76^{b,z} (10.38-27.05)	25.12^{ab,z} (14.71-42.90)	21.22^{ab,z} (15.13-29.77)	26.95^{ab,z} (19.21-37.81)
PV[1]	36.54^{a,z} (26.61-50.18)	19.02^{b,z} (10.98-32.94)	35.24^{ab,z} (19.07-65.14)	27.95^{ab,z} (18.95-41.22)	20.44^{b,yz} (13.86-30.15)
Myogenin					
AD	18.95^{a,yz} (11.42-31.46)	2.96^{b,y} (1.23-7.12)	32.32^{a,z} (12.11-86.25)	4.66^{b,y} (2.42-8.97)	3.79^{b,z} (2.04-7.05)
AV	16.01^{a,yz} (9.12-28.12)	3.90^{b,yz} (1.47-10.35)	24.21^{a,z} (6.87-85.31)	3.63^{b,y} (1.82-7.24)	5.20^{b,z} (2.61-10.36)
MV	14.30^{a,y} (8.85-23.10)	5.20^{b,yz} (2.26-11.93)	19.47^{a,z} (6.66-56.92)	4.33^{b,y} (2.40-7.79)	3.93^{b,z} (2.18-7.08)
PV	23.65^{a,z} (13.88-40.28)	7.16^{bc,z} (2.84-18.00)	24.36^{ab,z} (8.68-68.33)	8.38^{bc,z} (4.36-16.08)	6.03^{c,z} (3.14-11.58)

[1]AD = Anteriodorsal; AV = Anterioventral; MV = middle ventral; PV = Posterioventral.

$^{a-c}$Means and 95% confidence limits within a row (sampling region) without a common letter are significantly different ($P< 0.05$)

$^{x-z}$Means and 95% confidence limits within a column (line/WB affection status) without a common letter are significantly different ($P<0.05$)

Table 5. Decorin and insulin-like growth factor type 1 receptor (*IGF1R*) expression at four different locations within the pectoralis major muscle of three different genetic lines affected or unaffected by the wooden breast (WB) myopathy.

	Line A		Line B		Line C
Location	WB Affected	Unaffected	WB Affected	Unaffected	Unaffected
Decorin					
AD[1]	$7.10^{a,z}$ (4.80-10.50)	$1.29^{c,y}$ (0.65-2.54)	$4.94^{ab,z}$ (2.31-10.55)	$2.95^{b,y}$ (1.82-4.76)	$1.46^{c,y}$ (0.91-2.36)
AV[1]	$9.85^{a,z}$ (7.05-13.76)	$1.74^{c,yz}$ (0.97-3.10)	$9.05^{a,z}$ (4.74-17.29)	$3.46^{b,y}$ (2.30-5.21)	$1.63^{c,y}$ (1.08-2.45)
MV[1]	$9.33^{a,z}$ (6.77-12.85)	$3.04^{b,z}$ (1.75-5.30)	$6.15^{ab,z}$ (3.31-11.44)	$4.37^{b,yz}$ (2.95-6.47)	$3.74^{b,z}$ (2.53-5.54)
PV[1]	$8.00^{a,z}$ (5.83-10.98)	$3.06^{b,z}$ (1.77-5.29)	$6.87^{a,z}$ (3.72-12.68)	$6.05^{a,z}$ (4.11-8.92)	$2.68^{b,z}$ (1.82-3.95)
IGF1R					
AD	$24.64^{a,z}$ (19.46-31.18)	$13.73^{bc,yz}$ (9.13-20.65)	$19.03^{ab,y}$ (12.06-30.04)	$15.37^{b,x}$ (11.52-20.52)	$8.72^{c,y}$ (6.53-11.64)
AV	$24.73^{ab,z}$ (19.73-30.98)	$11.14^{c,y}$ (7.53-16.46)	$32.62^{a,z}$ (21.07-50.50)	$18.52^{b,xy}$ (14.05-24.42)	$11.11^{c,yz}$ (8.42-14.64)
MV	$27.99^{a,z}$ (22.50-34.83)	$17.62^{b,yz}$ (12.07-25.74)	$22.07^{ab,yz}$ (14.46-33.71)	$24.61^{a,yz}$ (18.83-32.17)	$15.68^{b,z}$ (11.99-20.49)
PV	$26.78^{a,z}$ (21.48-33.39)	$20.11^{ab,z}$ (13.73-29.46)	$23.57^{ab,yz}$ (15.38-36.13)	$31.79^{a,z}$ (24.27-41.64)	$14.92^{ab,z}$ (11.39-19.55)

[1]AD = Anteriodorsal; AV = Anterioventral; MV = middle ventral; PV = Posterior Ventral.

[a-c]Means and 95% confidence limits within a row (sampling region) without a common letter are significantly different ($P < 0.05$)

[x-z]Means and 95% confidence limits within a column (line/WB affection status) without a common letter are significantly different ($P<0.05$)

Figure 1. Samples for histology and gene expression were taken at four different locations within the pectoralis major. Samples were obtained from anterodorsal (AD), anteroventral (AV), middle-ventral (MV), and posteroventral (PV) positions. The histology samples are depicted in the figure by the rectangles and a corresponding sample used for gene expression was taken adjacent to each histology sample and is depicted by the circles. To obtain the AD sample, after all other samples were obtained the most anterior portion of the breast was cut to expose a portion of the p. major muscle approximately 2 cm underneath the AV sample.

Figure 2. Representative images of (A, C, E, G) wooden breast (WB) affected or (B, D, F, H) unaffected samples taken from (A, B) anterodorsal (AD), (C, D) anteroventral (AV), (E, F) middle-ventral (MV), and (G, H) posteroventral (PV) positions of pectoralis major muscles from line A broilers. EC = Endomysial Connective Tissue; ES = Endomysial Spacing; G = Giant Hypertrophic Fibers; M = Macrophage Infiltration; N = Fiber Necrosis; PC = Perimysial Connective Tissue; PS = Perimysial Spacing; S = Small Fibers with Centrally located Nuclei Scale Bar = 100 µm.

Figure 3. Representative images of (A, D, G, J) wooden breast (WB) affected or (B, C, E, F, H, I, K, L) unaffected samples taken from (A, B, D) anterodorsal (AD), (D, E, F) anteroventral (AV), (G, H, I) middle-ventral (MV), and (J, K, L) posteroventral (PV) positions of pectoralis major muscle from (A, B, D, E, G, H, J, K) line B and (C, F, I, L) line C broilers. EC = Endomysial Connective Tissue; ES = Endomysial Spacing; G = Giant Hypertrophic Fibers; M = Macrophage Infiltration; N = Fiber Necrosis; PS = Perimysial Spacing; S = Small Fibers with Centrally located Nuclei. Scale Bar = 100 µm.

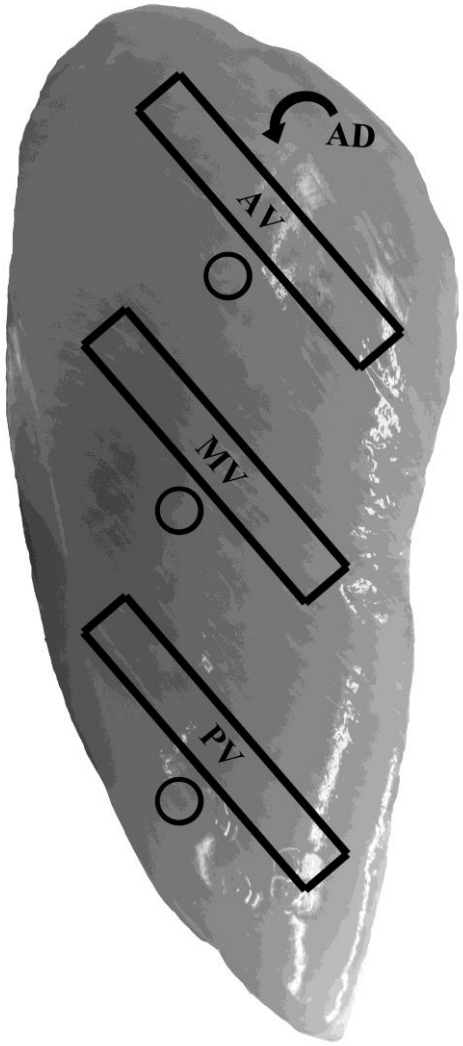

Figure 1.

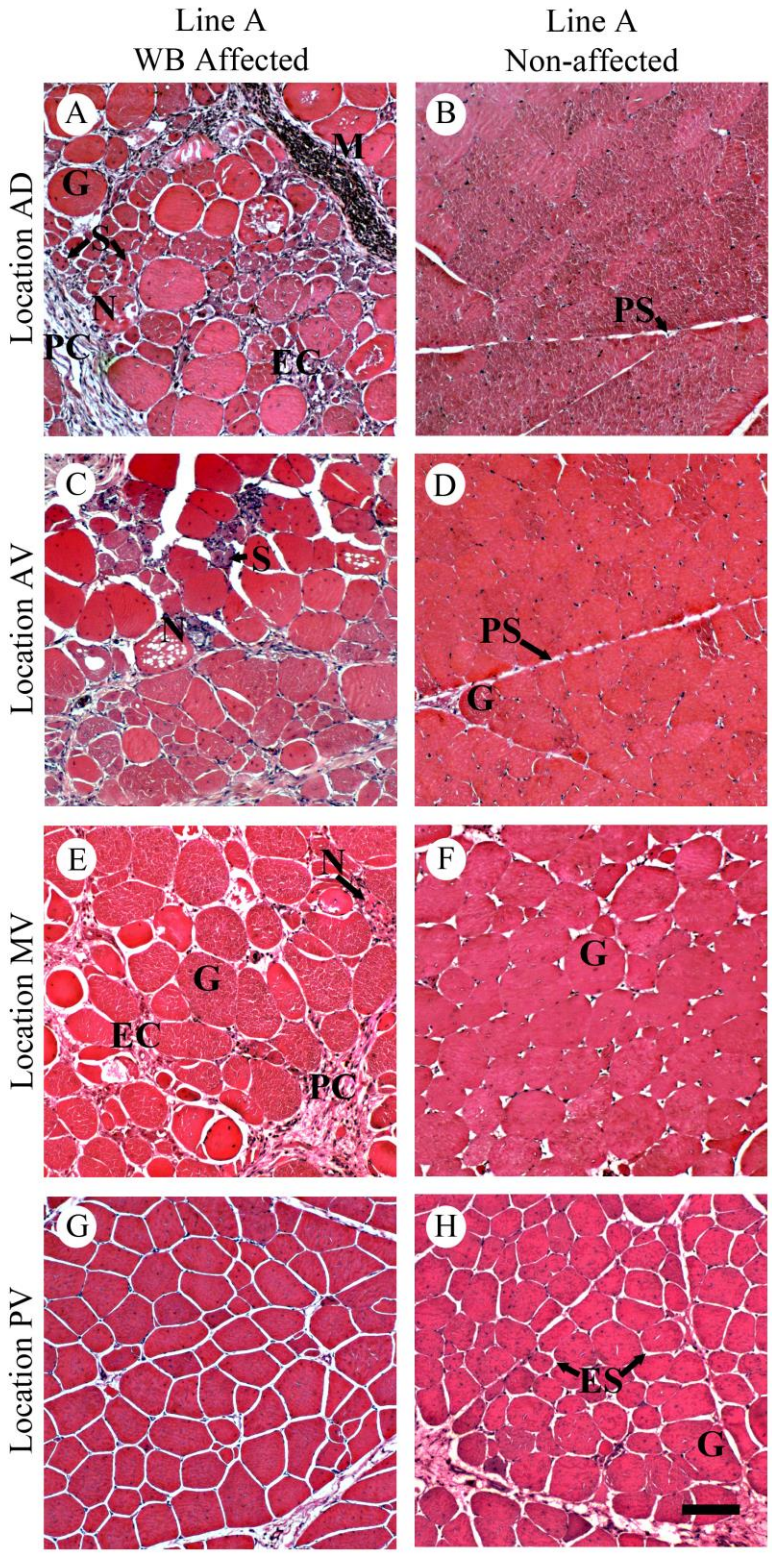
Line A
WB Affected
Line A
Non-affected
Location AD
Location AV
Location MV
Location PV
A
B
C
D
E
F
G
H
M
G
S
N
PC
EC
PS
S
N
PS
G
N
G
EC
PC
G
ES
G

Figure 2.

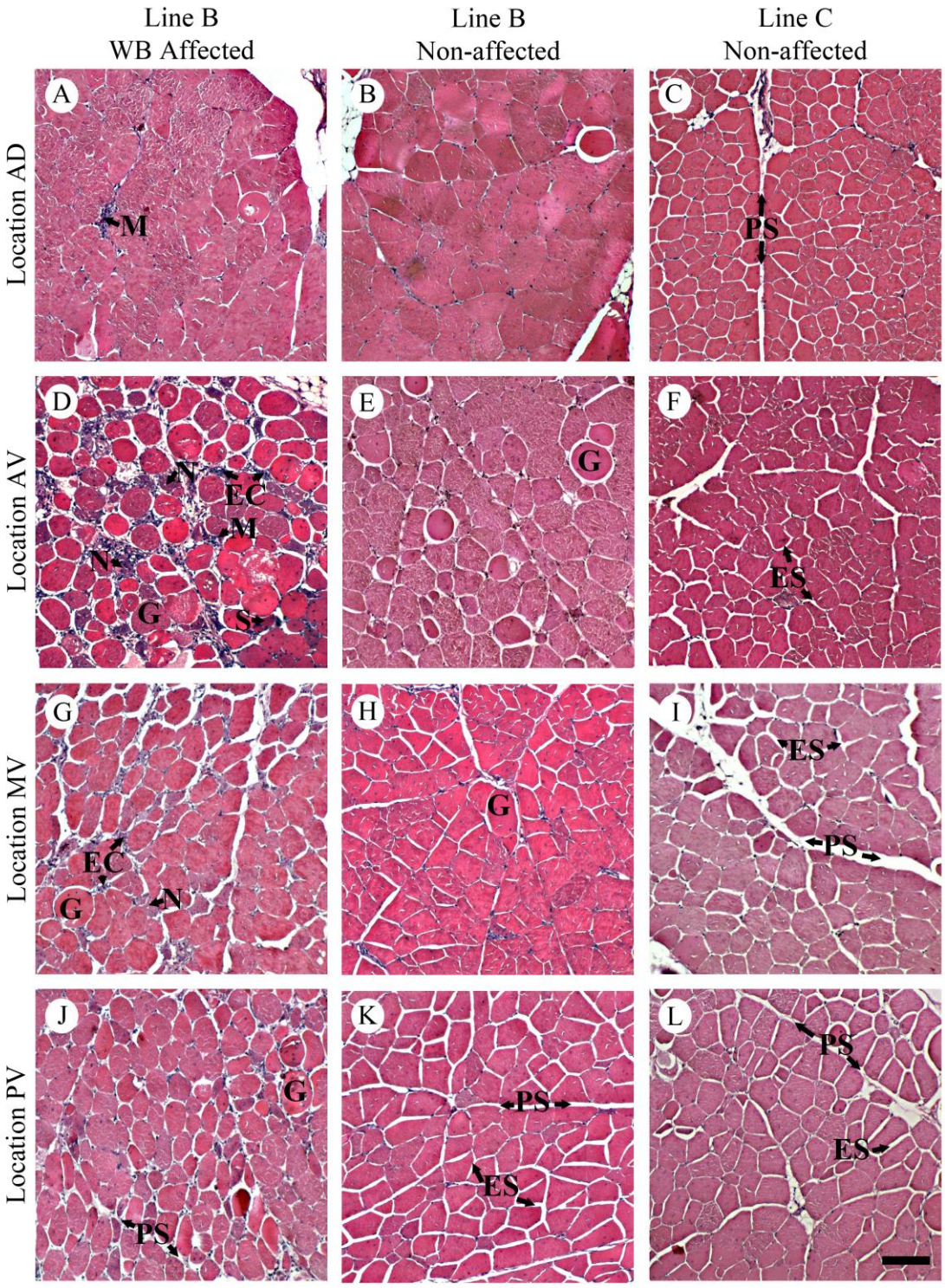
Line B
WB Affected
Line B
Non-affected
Line C
Non-affected
Location AD
Location AV
Location MV
Location PV
A
B
C
D
E
F
G
H
I
J
K
L
M
PS
N
EC
G
S
ES

Figure 3